arXiv:cond-mat/0003455v2 [cond-mat.stat-mech] 12 May 2000

A phenomenological glass model for vibratory granular compaction

D. A. Head*
Department of Physics and Astronomy, JCMB King's Buildings, University of Edinburgh, Edinburgh EH9 3JZ, United Kingdom

(February 6, 2008)

A model for weakly excited granular media is derived by combining the free volume argument of Nowak *et al.* [Phys. Rev. E **57**, 1971 (1998)] and the phenomenological model for supercooled liquids of Adam and Gibbs [J. Chem. Phys. **43**, 139 (1965)]. This is made possible by relating the granular excitation parameter Γ, defined as the peak acceleration of the driving pulse scaled by gravity, to a temperature-like parameter $\eta(\Gamma)$. The resulting master equation is formally identical to that of Bouchaud's trap model for glasses [J. Phys. I **2**, 1705 (1992)]. Analytic and simulation results are shown to compare favourably with a range of known experimental behaviour. This includes the logarithmic densification and power spectrum of fluctuations under constant η, the annealing curve when η is varied cyclically in time, and memory effects observed for a discontinuous shift in η. Finally, we discuss the physical interpretation of the model parameters and suggest further experiments for this class of systems.

PACS numbers: 05.40.-a, 45.70.Cc, 64.70.Pf

I. INTRODUCTION

It is well known that, with the appropriate driving and boundary conditions, granular matter can approximate each of the three major states of matter: gas, liquid and solid [1,2]. Conspicuous by its absence is a glass state; that is, a state where the relaxation times far exceed the observational timeframe [3–7]. However, it is becoming increasingly clear that the granular analogue of glass has been found in a recent series of experiments performed at the University of Chicago [8–11]. They measured the density of a system that was weakly perturbed or 'tapped' by the application of a driving pulse to the container. A first indication of glass-like relaxation processes came from analysis of the density $\rho(t)$, where t is the number of times the system had been tapped, which was found to increase only logarithmically slowly [8],

$$\rho(t) = \rho_{\mathrm{f}} - \frac{\Delta\rho}{1 + B\ln(1 + t/\tau)} \ . \tag{1}$$

The fitting parameters ρ_{f}, $\Delta\rho$, B and τ are functions of the control parameter Γ, defined as the peak acceleration of the driving pulse scaled by gravity, $\Gamma = a_{\max}/g$. Subsequent experiments in which Γ was varied during a run also behaved in a similar manner to glasses under a variable temperature [5–7,9–11], suggesting a relationship between Γ and some elusive temperature-like quantity.

Theoretical attempts to understand the experiments have ranged from the construction of toy microscopic models to higher level, coarse grained descriptions [12–25]. The general consensus has been that the slow relaxation is due to frustrated dynamics resulting from excluded volume effects. More insightful are the free volume arguments postulated by the Chicago group [9] and Boutreux and de Gennes [26], which derive the logarithmic compaction with only a small number of assumptions. Provocatively, these assumptions are also key components in established phenomenological models of glass-forming liquids, namely those of Adam and Gibbs [27] and Cohen and Turnbull [28], respectively. This further suggests that the analogy with glasses is a valid one. However, both of the granular free volume descriptions currently lack any mention of the experimental control parameter Γ and hence must be regarded as incomplete.

In this paper we demonstrate how one of the free volume arguments, namely that of the Chicago group, can be expanded into a full model that incorporates Γ. This is made possible by postulating a loose analogy between Γ in the granular system and temperature in supercooled liquids, and then using this analogy to incorporate elements of the Adam and Gibbs theory. The result of this process is a master equation for weakly excited granular media that is capable of reproducing a wide range of known experimental behaviour. The motivations behind this work are twofold. Firstly, by focusing on only a small number of physical mechanisms, the success of the model in emulating the experiments indicates that the dominant mechanisms may have been correctly identified. It is further hoped that this work may help to strengthen the relationship between granular matter and glasses. This second goal is easily achieved once we show that the derived master equation is identical to that of a simple glass model due to Bouchaud [29–32].

This paper is arranged as follows. In Sec. II the Chicago group's free volume argument is summarised and then expanded to a full model by importing elements of the Adam and Gibbs theory. The resulting master equation that describes the evolution of the system in time is specified. Numerical integration of this master equation, plus analytical results wherever possible, are compared to the experimental data in Sec. III. Of particular importance here is an explanation for the apparent contra-

diction between the experiments and any model based on the free volume approach, concerning the supposed Γ–dependence of the projected final density, $\rho_{\rm f}$ in (1). Further discussion on the physical interpretation of the model parameters is given in Sec. IV, as well as suggested ways in which the various assumptions behind the model may be more rigorously checked. Finally, we summarise our findings in Sec. V and make some tentative predictions for future experiments that may help to further elucidate the relevant physical mechanisms in granular compaction.

II. DESCRIPTION OF THE MODEL

The relationship between the Chicago group's free volume description and the Adam and Gibbs theory is that they both regard the dominant relaxation process to be the cooperative rearrangement of particles. The correspondence between the two theories can be taken further by postulating the existence of a temperature-like *noise* parameter $\eta(\Gamma)$ for weakly excited granular matter. This procedure forms the basis of our work, and is described in full below. For current purposes it is sufficient to provide a somewhat heuristic description of the model; a fuller discussion of the various parameters can be found in Sec. IV.

A. First principles derivation

The Chicago group's [9], and also Boutreux and de Gennes' [26], arguments employ the concept of the mean free volume per particle, here denoted $\bar{v_{\rm f}}$. For a system of N particles occupying a total volume V, $\bar{v_{\rm f}}$ is defined as

$$\bar{v_{\rm f}} = \frac{V - V_{\rm min}}{N} = v_{\rm g}\left(\frac{1}{\rho} - \frac{1}{\rho_{\rm max}}\right) \ , \qquad (2)$$

where $v_{\rm g}$ is the volume of a single particle and ρ is the volume fraction $Nv_{\rm g}/V$. Units are chosen so that the density of a single grain is unity, hence ρ is also the density of the system. Following [26], $\rho_{\rm max} \equiv Nv_{\rm g}/V_{\rm min}$ is identified with the most compact state possible in a disordered system, *i.e.* the random close-packing limit. In what follows we shall fix $\rho_{\rm max} = 0.64$, believed to be the random close packed density for a system of monodisperse spheres [33].

The Chicago group postulated that the compaction process is dominated by the cooperative rearrangement of local domains of particles. If z is the number of particles in a region that can rearrange independently of its environment, they argued there is a lower cut-off

$$z \geq z^* = a\,\frac{v_{\rm g}}{\bar{v_{\rm f}}} \qquad (3)$$

below which there is not enough free volume available to allow reconfiguration. Roughly speaking, z^* is the number of particles that, by adding up their individual free volumes, can make a single 'hole' big enough to allow exactly one particle to fit through. The explicit dependence of z^* on ρ is found by combining (2) and (3),

$$z^* = a\left(\frac{1}{\rho} - \frac{1}{\rho_{\rm max}}\right)^{-1} \ . \qquad (4)$$

By assuming that the density increases at a rate proportional to e^{-z^*}, it is now possible to derive the logarithmic compaction law $\rho(t) \sim -1/\ln(t)$ [9].

As mentioned in the introduction, the theory just outlined is incomplete as it does not incorporate the experimental control parameter Γ. In an attempt to resolve this deficiency, we observe that a similar description for cooperative relaxation is also central to the theory proposed by Adam and Gibbs for structural relaxation in supercooled liquids [27]. An intermediate stage of their calculations is of interest here, namely that the relaxation rate W can be expressed as a function of temperature T as

$$W(T) \propto \exp\left(-\frac{z^*\Delta E}{k_{\rm B}\,T}\right) \ , \qquad (5)$$

where ΔE is the free energy barrier per particle, $k_{\rm B}$ is Boltzmann's constant and z^* is again the smallest number of particles that can rearrange independently of their environment (which was ultimately related to the configurational entropy).

The principle assumption behind our current work is that an expression analogous to (5) also holds for weakly excited granular media. More precisely, we propose that a region with local density ρ reconfigures at a rate

$$W(\rho,\Gamma) \propto \exp\left(-\frac{z^*(\rho)\Delta E}{\eta(\Gamma)}\right) \ , \qquad (6)$$

where z^* is related to ρ via (4). ΔE can be interpreted as a gravitational potential energy barrier per particle, and $\eta(\Gamma)$ gives some measure of the degree of excitation of the system. Note that although $\eta(\Gamma)$ plays the role of $k_{\rm B}\,T$, we stop short of referring to it as a 'granular temperature' and instead regard it as a noise parameter which is *defined* by (6), with the only restriction that $\eta(\Gamma)$ should be a monotonic increasing function of Γ. In what follows $\eta(\Gamma)$ is essentially treated as a fitting parameter. The physical meaning of $\eta(\Gamma)$ and ΔE is discussed further in Sec. IV.

To fully specify the model, some rule is required that gives the density of a region after it has reconfigured. In general this will depend on its density before reconfiguration as well as $\eta(\Gamma)$, but for simplicity we shall ignore such considerations here and simply assume that the density after reconfiguration is given by the fixed probability density function $\mu'(\rho)$. Specifically, $\mu'(\rho)\,\mathrm{d}\rho$ is the probability that a region 'falls' into a configuration with a density in the range $[\rho, \rho + \mathrm{d}\rho)$. The prior distribution

$\mu'(\rho)$ (re-expressed in terms of the total energy barrier E – see below) will play a central role in our model, although it shall be demonstrated that, over timescales relevant to the experiments, the model is essentially robust to the particular choice of $\mu'(\rho)$. This is fortuitous, as the precise form of $\mu'(\rho)$ is unknown and we have instead considered a range of plausible functional forms.

B. Summary of the model

Since the reconfiguration rate $W(\rho,\Gamma)$ given in (6) depends on ρ only via the total energy barrier $E = z^*(\rho)\Delta E$, it is convenient to now make the change of variables $\rho \to E$, where

$$E = z^*\Delta E = A\left(\frac{1}{\rho} - \frac{1}{\rho_{\max}}\right)^{-1} , \tag{7a}$$

$$A = a\,\Delta E , \tag{7b}$$

which is one-to-one and hence invertible for all $\rho \in [0,\rho_{\max})$ and $E \in [0,\infty)$. Thus, in what follows, the state of the system at any given time t will in the first place be defined by the distribution of energy barriers $P(E,t)$, and only then shall the mean density $\rho(t)$ be found by inverting the mapping (7) and averaging over $P(E,t)$, *i.e.*

$$\rho(t) = \int_0^\infty \frac{P(E,t)}{\frac{A}{E} + \frac{1}{\rho_{\max}}}\,\mathrm{d}E . \tag{8}$$

Note that, in principle, small values of E should be disallowed to reflect the fact that low density configurations are not mechanically stable and will not arise. For the sake of simplicity we choose to ignore this subtlety here.

The master equation for $P(E,t)$ can be derived as follows. The rate at which a region with a local barrier $E(\rho)$ reconfigures is given by $\omega_0\,\mathrm{e}^{-E/\eta}$, where the constant ω_0 fixes the timescale. After reconfiguring, the region falls into a state with a new barrier $E_{\rm new}$ with a probability $\mu(E_{\rm new})$, where $\mu(E)$ is just $\mu'(\rho)$ after the change of variables, $\mu(E)\mathrm{d}E = \mu'(\rho)\mathrm{d}\rho$. Assuming that the number of taps t can be well approximated as a continuous variable, $P(E,t)$ evolves in time according to

$$\frac{1}{\omega_0}\frac{\partial P(E,t)}{\partial t} = -\,\mathrm{e}^{-E/\eta}P(E,t) + \omega(t)\,\mu(E) , \tag{9a}$$

$$\omega(t) = \int_0^\infty \mathrm{e}^{-E/\eta}P(E,t)\,\mathrm{d}E . \tag{9b}$$

The first and second terms on the right hand side of (9a) correspond to regions with barriers E before and after a reconfiguration event, respectively. Conservation of probability is ensured by $\omega(t)$, which is the total rate of reconfiguration events at time t.

Remarkably, the coupled equations (9a) and (9b) are *identical* to the trap model of Bouchaud, which is known to qualitatively reproduce many features of spin glasses and supercooled liquids [29–32]. Thus the model we have derived can also be viewed as Bouchaud's trap model, with a mapping from the energy barrier E to density ρ that is reached via the two-stage process of first assuming that E is proportional to the smallest region that can rearrange independently of its environment, *à la* Adam and Gibbs, and then using the Chicago group's free volume argument to relate the size of this region to its density. The relationship with Bouchaud's trap model is useful as it allows known analytical results to be transferred to this application, as described in the following section.

III. COMPARISON TO THE EXPERIMENTS

In this section we compare the predictions of the model to the experimental results given in [8–11]. The general procedure employed throughout was to numerically integrate $P(E,t)$ in time according to the master equation (9) from an initial state $P(E,0)$, using the method described in Appendix A. Ideally $P(E,0)$ would be chosen to mimic the distribution of density in the apparatus after the preparation phase, but since such information is not available we have instead employed the natural choice of $P(E,0) = \mu(E)$, which formally corresponds to an instantaneous 'quench' from $\eta = \infty$. No significant deviations are expected for other initial conditions after an initial transient. Once $P(E,0)$ was fixed, the constant A in (7) was chosen by trial-and-error to give an initial density close to the experimental value $\rho(0) \approx 0.58$. The density $\rho(t)$ was extracted at regular intervals by numerical evaluation of (8).

Each simulation was repeated for two different choices of $\mu(E)$, namely an exponential $\mu(E) = \frac{1}{E_0}\mathrm{e}^{-E/E_0}$ and a Gaussian $\mu(E) = \sqrt{2/\pi\sigma^2}\mathrm{e}^{-E^2/2\sigma^2}$, where without loss of generality we now choose units such that $E_0 = \sigma = 1$. Other $\mu(E)$ were also considered for the compaction under constant η described in Sec. III A and were found to give the same behaviour for $t \lesssim 10^4$ taps, indicating that the model is robust to the particular choice of $\mu(E)$ over the experimental timeframe. However, this robustness does *not* extend to the $t \to \infty$ limit, where it is already known that different $\mu(E)$ can give qualitatively different behaviour. This is discussed thoroughly in [32], but in brief, an exponential tail $\mu(E) \sim \mathrm{e}^{-E}$ gives rise to a *glass transition* at $\eta = 1$, in the sense that an equilibrium solution only exists for $\eta > 1$. This can be seen by simply setting $\partial P/\partial t = 0$ in the master equation (9),

$$P_{\rm eqm}(E) \equiv \lim_{t\to\infty} P(E,t) = \omega(\infty)\,\mathrm{e}^{E/\eta}\mu(E) , \tag{10}$$

which is not normalisable for $\eta \le 1$ if $\mu(E) \sim \mathrm{e}^{-E}$, and hence equilibrium cannot be reached. By contrast, if $\mu(E)$ decays more rapidly than exponentially, *e.g.* if it has a Gaussian tail, then an equilibrium solution exists for all $\eta > 0$, although the equilibration time may be excessively large for small η. Note that this

model quite generally predicts that the limiting density $\rho_\infty = \lim_{t\to\infty}\rho(t)$ is a monotonic decreasing function of η. A proof of this is given in Appendix B.

A. Constant excitation intensity

Simulation results for the mean density $\rho(t)$ over a range of η is given in Fig. 1. Also given are fits to the empirical law (1), demonstrating that it is well obeyed with either an exponential and Gaussian $\mu(E)$. We have also checked and found similar logarithmic behaviour for a selection of other $\mu(E)$, such as uniform on $[E_0, E_1]$, both with $E_0 = 0$ and $E_0 > 0$, Gaussian with a non-zero mean, Cauchy, and exponential limited to the range $[E_0, E_1]$. However, logarithmic relaxation is *not* expected for pathological $\mu(E)$ such as $\delta(E - E_0)$ or $\exp(-\mathrm{e}^E)$.

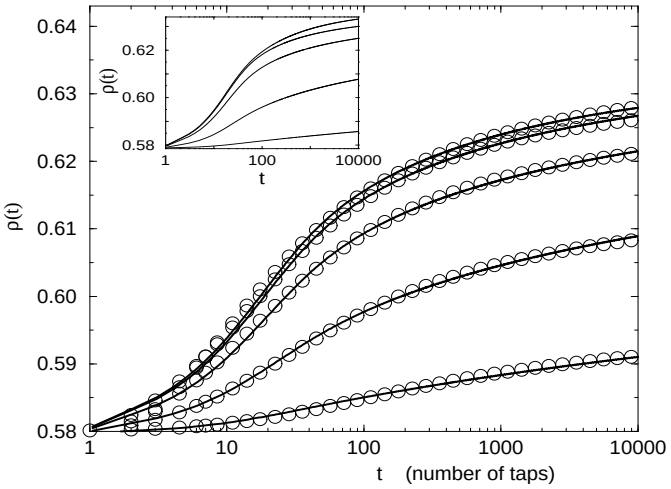

FIG. 1. Plot of $\rho(t)$ versus t on log-linear axes for a Gaussian $\mu(E) = \sqrt{2/\pi}\mathrm{e}^{-E^2/2}$ with $\rho_{\max} = 0.64$, $\omega_0 = 0.1$ and $A = 0.053$. From bottom to top, the lines correspond to $\eta = 0.005$, 0.03, 0.1, 0.2 and 0.3 respectively. The circles are fits to the empirical law (1). *(Inset)* The corresponding results for an exponential $\mu(E) = \mathrm{e}^{-E}$ and $A = 0.05$, with $\eta = 0.002$, 0.02, 0.1, 0.2 and 0.5 .

The logarithmic behaviour can be understood by considering the scaling solution to the master equation (9) already found by Monthus and Bouchaud [32]. They demonstrated that, after a short transient, $P(E,t)$ can be expressed in terms of a single scaling variable u as

$$P(E,t) = \frac{1}{\eta}\, u\, \phi(u)\,, \qquad u = \frac{\mathrm{e}^{E/\eta}}{\omega_0\, t}\ . \tag{11}$$

Strictly speaking this is only true for an exponential $\mu(E)$ below the glass point, but it was also demonstrated that a Gaussian $\mu(E)$ admits a similar scaling solution until a time $t^* \sim \omega_0^{-1}\exp(1/\eta^2)$, which may lie well beyond the experimental timeframe when η is small. The physical picture underlying this scaling behaviour is that the sizes of the cooperatively rearranging regions, which are proportional to $E = \eta\ln(\omega_0 t u)$, are increasing logarithmically in time. A logarithmic increase in domain size has also been found in the Tetris model [15].

Over timescales for which the scaling solution (11) holds, the density can be expressed in terms of $\phi(u)$ by changing variables from E to u in (8),

$$\frac{\rho(t)}{\rho_{\max}} = 1 - \int_{\frac{1}{\omega_0 t}}^{\infty} \frac{\phi(u)}{1 + \dfrac{\eta}{A\rho_{\max}}\ln(\omega_0 t u)}\,\mathrm{d}u\ . \tag{12}$$

The similarity of this expression to the empirical law (1) is striking. The primary difference is that here we must integrate over a distribution of u, which will in general introduce corrections to the simple logarithmic law. The simulation results in Fig. 1 demonstrate that any such corrections are at most small.

The form of the theoretical prediction (12) makes it difficult to calculate the fitting parameters $\Delta\rho$, B and τ in the empirical law (1). However, one parameter that can trivially be fixed is the projected final density ρ_{f}, which is always equal to $\rho_{\max}$ here, regardless of $\eta(\Gamma)$. In contrast, the experiments seem to indicate that ρ_{f} is a non-monotonic function of Γ [8]. There is no easy way to resolve this discrepancy. For instance, one cannot simply assume that $\rho_{\max}$ is itself a function of Γ, *i.e.* $\rho_{\max} = \rho_{\max}(\Gamma)$. Quite apart from the conceptual difficulties this would invoke for the physical meaning of $\rho_{\max}$, it would allow situations in which *negative* free volume could arise, for instance by first allowing a system to relax arbitrarily close to $\rho_{\max}(\Gamma)$ and then suddenly changing to a Γ' for which $\rho_{\max}(\Gamma') < \rho_{\max}(\Gamma)$. By definition, $\bar{v_{\mathrm{f}}}$ would then be negative. Note that this contradiction is not specific to this model but will arise whenever the definition of free volume (2) is used.

We believe the solution to this problem lies in the range of t over which the data fitting has been performed. As mentioned previously, the scaling solution (11), and hence the logarithmic relaxation, only applies after a short transient, typically $t \gtrsim 10^2 - 10^3$ taps. However, we have found that it is still possible to attain a very reasonable fit to the empirical law over the whole range $0 \le t \le 10^4$, but *only at the expense of predicting the wrong* ρ_{f}. This is clearly demonstrated in Fig. 2, which shows that a fit that works well for $0 \le t \le 10^4$ fails when extrapolated to larger t, whereas fixing $\rho_{\mathrm{f}} = \rho_{\max}$ gives an initially poorer fit but recovers the correct asymptotic behaviour. Transferring this insight to the experiments suggests that discarding the first 1-10% of the experimental data points and then repeating the fitting procedure would result in a similar logarithmic compaction law as before, but with ρ_{f} independent of Γ. The various time regimes in this model are summarised schematically in Fig. 3.

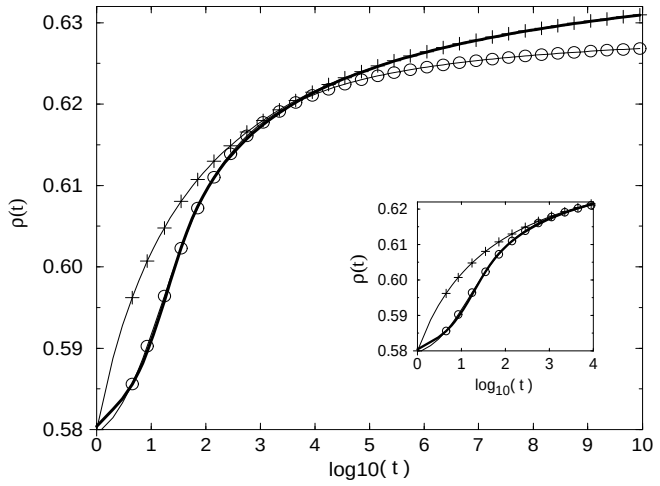

FIG. 2. Comparison between different choices of fitting parameters over different ranges of t. The thick line is the density $\rho(t)$ for a Gaussian $\mu(E)$ at $\eta = 0.1$ with $\rho_{\max} = 0.64$. The circles correspond to the fit $\rho(t) = 0.63 - 0.053/(1+2.3\ln(1+t/16))$ and the crosses correspond to $\rho(t) = \rho_{\max} - 0.06/(1+0.24\ln t)$. *(Inset)* The same plots over the experimental timeframe $1 \le t \le 10^4$.

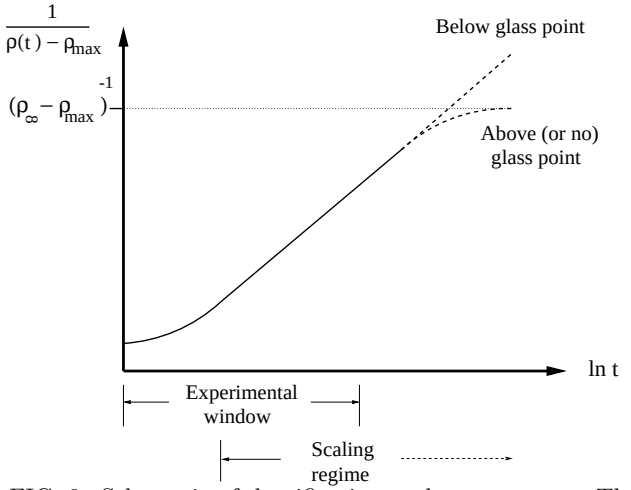

FIG. 3. Schematic of densification under constant η. The line becomes straight, indicating that the density is logarithmically increasing towards $\rho_{\max}$, once the system enters into the scaling regime, which overlaps with the experimental window. The scaling regime continues indefinitely if $\mu(E) \sim \mathrm{e}^{-E/\eta_{\mathrm{g}}}$ and $\eta \le \eta_{\mathrm{g}}$. For $\eta > \eta_{\mathrm{g}}$, or for a $\mu(E)$ with a tail that decays faster than exponentially, the scaling behaviour ceases at some late time and the density reaches its equilibrium density $\rho_\infty < \rho_{\max}$.

B. Annealing curve

Further insight into the nature of the system's relaxation properties can be gained by allowing the tap intensity to vary in time, which roughly corresponds to varying the temperature in other slowly relaxing systems [5,6]. Two time-dependencies will be considered in this paper. The first is the 'annealing curve,' which was experimentally attained by cyclically ramping Γ in a stepwise fashion between some high value $\Gamma = \Gamma_1$ and $\Gamma = 0$ [9,10]. Slowly decreasing Γ removes low density local configurations without creating many new ones, hence the term 'annealing.' The second protocol for varying Γ will be investigated in the next subsection.

The annealing curve for this model is obtained by allowing η to smoothly vary from 0 to some value η_1 to 0 to η_1 again, where the duration of each leg is denoted by t_{leg}. Simulation results for $t_{\mathrm{leg}} = 10^6$ are given in Fig. 4. The experimental annealing curve has a similar shape, except that the initial density increase for small Γ is noticeably slower than that for small η [9]. This may simply be due to a non-trivial mapping from Γ to η, as discussed in Sec. IV. Note that the second and third legs in Fig. 4 form a reversible curve which is nonetheless out of equilibrium for small η. Observe also the presence of a narrow hysteresis loop, which is also present in microscopic models [14,17,22] but has never been systematically searched for in experiments. The area of this hysteresis loop decreases for slower cooling rates, as demonstrated in Fig. 5.

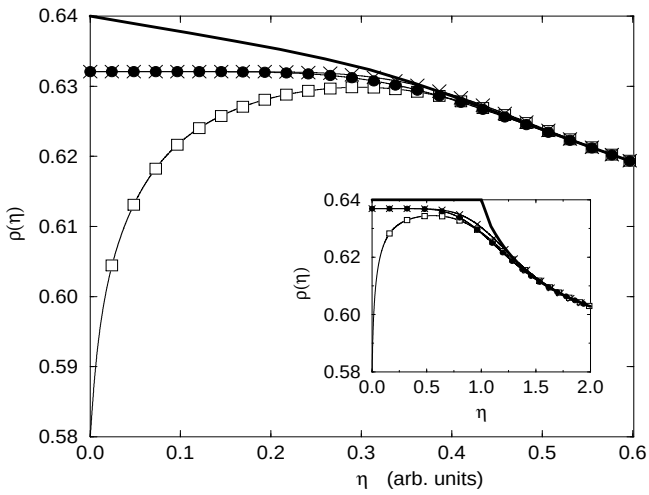

FIG. 4. The annealing curve for a Gaussian $\mu(E)$. The symbols refer to the initial increase in η up to $\eta = 0.6$ (open squares), the decrease to $\eta = 0$ (filled circles) and the second increase (crosses). For each leg, η was varied smoothly over $t_{\mathrm{leg}} = 10^6$ taps. The thick line is the equilibrium density. *(Inset)* The same for an exponential $\mu(E)$ over a range of η that includes the glass point.

To interpret these results in a glassy context, recall that the initial conditions were chosen to conform to the equilibrium state at $\eta = \infty$, *i.e.* $P(E,0) = P_{\mathrm{eqm}}(E)|_{\eta=\infty} = \mu(E)$. This would be valid if the ini-

tial low density configuration in the experiments corresponded to an equilibrium state for very large tapping intensity Γ, which seems plausible. Thus the start of the first leg corresponds to a rapid *quench* from high η to $\eta \approx 0$, leaving the system far from equilibrium. The rate of compaction is initially rapid but slows as the density, and hence the relaxation times, increase. For sufficiently high η, the density reaches and starts to follow the equilibrium curve, rapidly erasing the memory of its history. As η is lowered a second time, this time corresponding to a slow quench, the system remains near equilibrium until some value η_0 (which depends on the cooling rate) when the relaxation time rapidly increases and the system essentially freezes. Thus the difference between the first and third legs in Fig. 4 can be understood as the recovery from a rapid and slow quench, respectively.

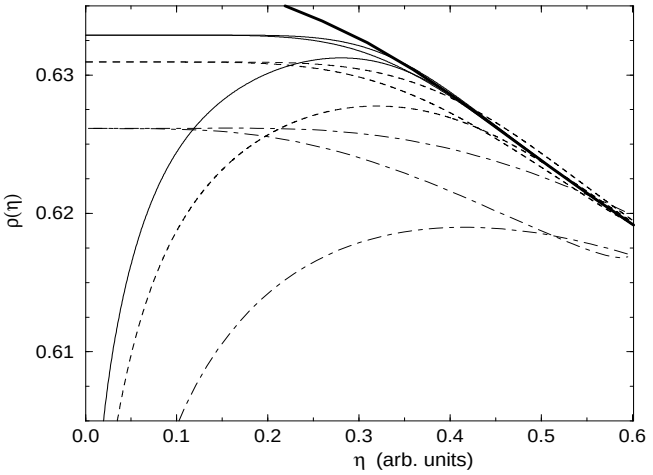

FIG. 5. Variation of the annealing curves with cooling rate for a Gaussian $\mu(E)$. Results are given for a total time per leg of $t_{\rm leg} = 10^7$ (thin solid line), 10^5 taps (dashed line) and 10^3 taps (dot-dashed line). The second and third legs are reversible for $t_{\rm leg} \gtrsim 10^5$. The thick line is the equilibrium density.

C. Shift in the excitation intensity

Recent experiments have investigated the effect of allowing Γ to 'shift' from a constant value Γ_0 to another constant value Γ_1 at a given time t_0 [11]. It was found that the system evolved in a way that depended on its history as well as its current density and excitation intensity Γ, representing a form of memory akin to that in glassy systems [5,6]. Plotted in Fig. 6 are the corresponding results for this model, where $\eta = \eta_0 = 0.5$ until $t = t_0 = 50$ taps, when it changes to $\eta_1 = \eta_0 + \Delta\eta$. The sign of the initial density change is opposite to the sign of $\Delta\eta$, as in the experiments, although this is not entirely general and the behaviour is reversed if t_0 is too small. Also shown in the inset is the case when η is changed from different η_0 to the same value $\eta_1 = 0.3$ when the density reaches a predetermined value. Again there is qualitative agreement with the experiments.

The analogy with glass systems suggests that the timescale of the response to a shift in η at t_0 should scale with t_0 in some manner [34]. With this insight, we now make the following prediction, in the hope it may be tested experimentally. Let $\Delta\rho(t-t_0)$ be the difference in density at time t between the perturbed system and an unperturbed one, *i.e.* one with $\Delta\eta = 0$. Plotted in Fig. 7 is $\Delta\rho(t-t_0)$ for a shift from a low to a high η at times $t_0 = 10^3$, 10^4, 10^5, 10^6 and 10^7. In each case there is a well-defined time for the peak response $t^{\rm resp}$, which increases with t_0. Known results for the trap model with an exponential $\mu(E)$ suggest that $t^{\rm resp} \sim t_0^{\eta_0/\eta_1}$, where the exponent is independent of t_0 [35]. We find this to be a good first approximation to our data, as demonstrated by the inset to Fig. 7, although there are corrections arising from the non-linear mapping from E to ρ, which distorts the underlying scaling behaviour in E. There are also additional small corrections when using a Gaussian $\mu(E)$.

Finally, the experiments briefly investigated what happens when Γ is allowed to return to its initial value after δt taps at a higher value Γ_1 [11]. For comparison, the equivalent results from this model are given in Fig. 8. The observed trend is in accord with the experimental observations. A full study of this variation in $\eta(t)$ for all η_0, η_1, t_0 and δt is beyond the scope of this paper and will not be discussed further here.

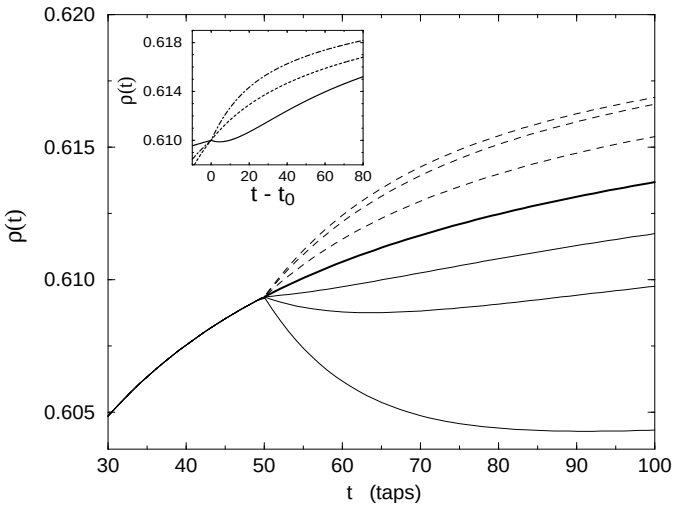

FIG. 6. Response to a shift from $\eta = 0.5$ to $\eta = 0.5 + \Delta\eta$ at a time $t = 50$ for a Gaussian $\mu(E)$. From top to bottom, the lines refer to $\Delta\eta = -0.3$, -0.2 and -0.1 (dashed lines), 0 (thick line) and 0.1, 0.2 and 0.5 (thin solid lines). *(Inset)* Here $\eta = 0.1$ (solid line), 0.3 (dashed line) or 0.5 (dot-dashed line) until the first time t_0 when $\rho(t_0) \geq 0.61$, afterwhich η is fixed at 0.3 in each case.

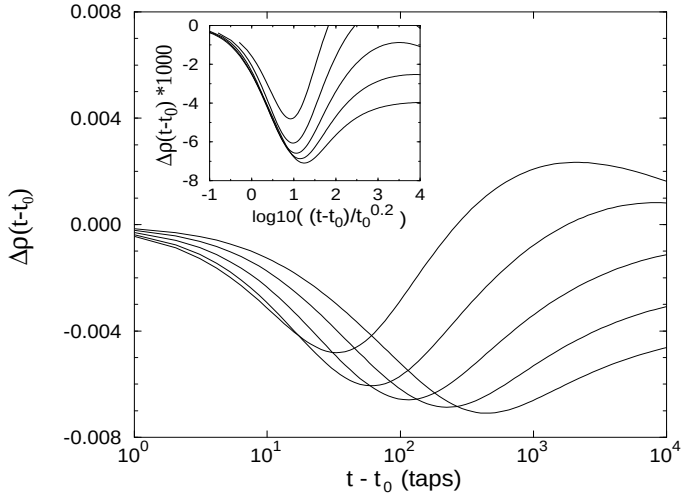

FIG. 7. Response to a shift from $\eta = 0.1$ to $\eta = 0.5$ at a time t_0 for a Gaussian $\mu(E)$, where $\Delta\rho(t - t_0)$ is the density difference between perturbed and unperturbed systems. From top the bottom on the right hand side, the lines refer to $t_0 = 10^3$, 10^4, 10^5, 10^6 and 10^7 respectively. An exponential $\mu(E)$ behaves similarly. *(Inset)* The same data plotted against $(t - t_0)/t_0^{\alpha}$, where $\alpha = 0.1/0.5$ is the ratio of η before and after the shift.

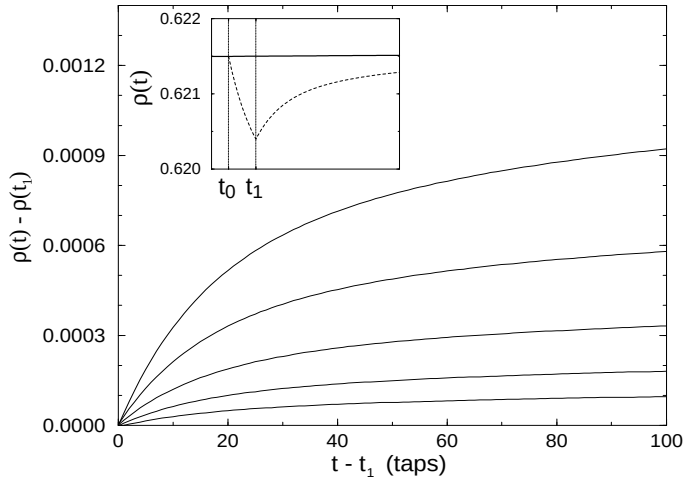

FIG. 8. Plot of the recovery from a short time at a higher η for a Gaussian $\mu(E)$. Here the system has been relaxed for a time $t_0 = 10^4$ taps at $\eta = 0.1$, then held at $\eta = 0.3$ until $t_1 = t_0 + \delta t$ when it reverts back to $\eta = 0.1$ again. From bottom to top, the lines refer to $\delta t = 1$, 2, 4, 8 and 16, respectively. *(Inset)* The raw data for $\delta t = 16$ (dashed line) compared to the unperturbed system (solid line).

D. Fluctuations and power spectra

In a finite system the density in equilibrium is not constant but fluctuates about its mean value. To investigate density fluctuations in this model, a different version of the code was employed which explicitly simulates a system consisting of N separate subsystems (details given in Appendix A). Fig. 9 shows the probability distribution $Q(\Delta\rho)$ of fluctuations $\Delta\rho \equiv \rho(t) - \rho_{\rm modal}$ for $N = 500$ and different η. To first approximation $Q(\Delta\rho)$ is Gaussian, but it is slightly skewed towards lower densities, becoming more so as η is lowered. The skewness arises from the non-linear mapping from E to ρ, which exaggerates fluctuations to lower densities whilst suppressing those to high densities. There is also a cut-off for very large $|\,\Delta\rho\,|$, when $P(E,t)$ has deviated significantly from $P_{\rm eqm}(E)$. The experiments exhibited Gaussian fluctuations with some anomalous deviations for $\Delta\rho > 0$ [9]; this is discussed below.

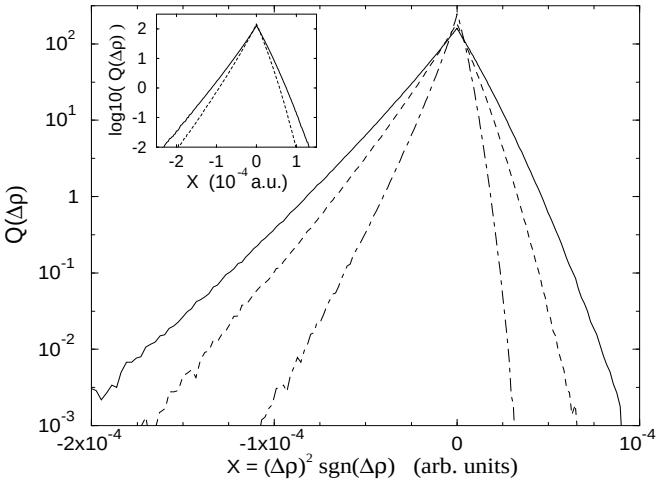

FIG. 9. Fluctuations around the modal density $\rho_{\rm modal}$ in equilibrium for an $N = 500$ element system with a Gaussian $\mu(E)$. $Q(\Delta\rho)$, the probability of a fluctuation $\Delta\rho = \rho(t) - \rho_{\rm modal}$, is plotted against $X = (\Delta\rho)^2 {\rm sgn}(\Delta\rho)$ on a log-linear plot, which would give a symmetrical triangle if $Q(\Delta\rho)$ was Gaussian. The different lines refer to $\eta = 1$ (solid), $\eta = 0.8$ (dashed) and $\eta = 0.6$ (dot-dashed). *(Inset)* The same for an exponential $\mu(E)$ with $\eta = 2$ (solid line) and $\eta = 1.6$ (dashed line).

The power spectra $S(f)$ of density fluctuations in equilibrium for various η and a Gaussian $\mu(E)$ is given in Fig. 10. $S(f) \sim 1/f^2$ for f greater than a high frequency shoulder $f_{\rm H}$, where $f_{\rm H}$ is only weakly dependent on η, although it should be stressed that this model focuses on cooperative relaxation modes and is not intended to describe the high frequency, single particle dynamics. For low frequencies, $S(f)$ appears to obey non-trivial power law behaviour $S(f) \sim 1/f^{\delta}$, where the exponent δ can be *very approximately* fitted to $\delta \approx 1 - \eta$ over the range

$10^{-5} < f < 10^{-3}$. However, the analysis given in Appendix C shows that this is not the true asymptotic behaviour and $S(f) \to 1/f^0$ as $f \to 0$. The crossover to $1/f^0$ behaviour occurs around a low frequency shoulder $f_{\rm L}$, where $f_{\rm L} \to 0$ rapidly as $\eta \to 0$. For an exponential $\mu(E)$ there is only one shoulder frequency separating the high frequency, $1/f^2$ regime from a low frequency regime in which $S(f) \sim 1/f^{\delta}$, where $\delta = 2 - \eta$ for $1 < \eta < 2$ and $\delta = 0$ for $\eta \geq 2$. Note that there is no $1/f^0$ region for $\eta < 2$, even though the system is in equilibrium. This apparent anomaly is explained in Appendix C.

In the experiments, the power spectra were found to obey non-trivial power law behaviour $S(f) \sim 1/f^{\delta}$, with $\delta = 0.9 \pm 0.2$, between two corner frequencies $f_{\rm L}$ and $f_{\rm H}$ that both decreased as Γ was lowered [9]. More complex behaviour was observed for larger Γ towards the bottom of the apparatus. The results from this model are in partial agreement; for instance, it is still one of few that can exhibit a $1/f^{\delta}$ regime with $\delta \approx 1$ (see also [21]). There are some discrepancies, but these may simply be due to processes not currently incorporated into the model, such as single particle dynamics or the existence of metastable, high-density crystalline domains.

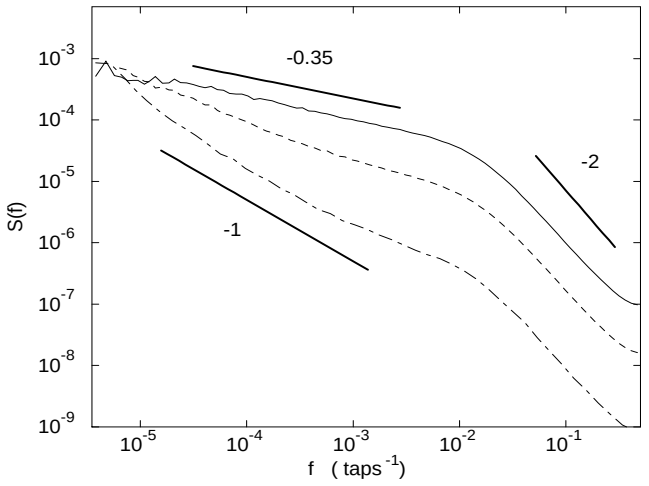

FIG. 10. $S(f)$, the power spectrum of frequency f, for an $N = 500$ system and a Gaussian $\mu(E)$, at $\eta = 0.6$ (solid line), $\eta = 0.4$ (dashed line) and $\eta = 0.2$ (dot-dashed line, also vertically shifted by a factor of 500 for clarity). Each $S(f)$ was calculated over $\approx 10^8$ points. The slopes of the thick line segments are indicated. To speed convergence, the initial configuration was chosen as the known equilibrium state $P_{\rm eqm}(E)$ for $N = \infty$ (10), although the $\eta = 0.2$ system was still evolving towards its slightly different finite N equilibrium state during the run. This accounts for the anomalous steep slope for small f.

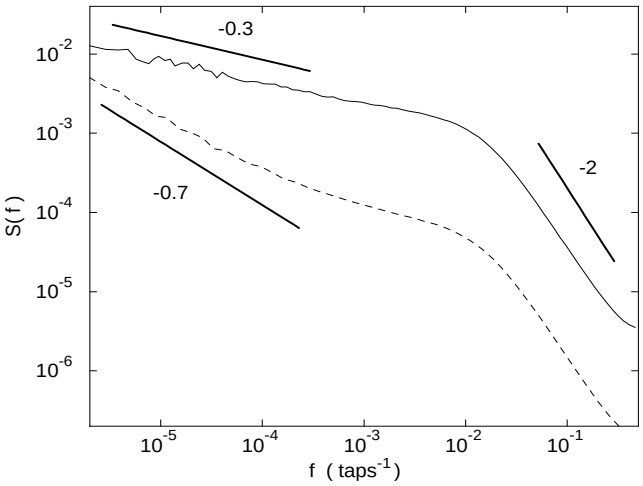

FIG. 11. $S(f)$ in equilibrium for an exponential $\mu(E)$ and $N = 500$, with $\eta = 1.7$ (solid line, also shifted vertically by a factor of 10) and $\eta = 1.3$ (dashed line). The analytical predictions from Appendix C are indicated by the thick line segments.

IV. DISCUSSION OF THE MODEL PARAMETERS

Given the success of this model in reproducing the experimental phenomenology, it is natural to ask if its principle assumptions can be placed on a firmer foundation. In particular, a number of parameters introduced in Sec. II A have so far been treated somewhat heuristically. To redress the balance, we now discuss the physical interpretation of some of these parameters. A more thorough analysis may be possible by detailed comparison with a microscopic model, for instance.

1. The noise parameter $\eta(\Gamma)$

It was stressed during the derivation of this model that the noise parameter η need not bear any relation to the concept of granular temperature [36,37]. By the same token, the use of the term 'equilibrium' to describe the statistical steady state merely refers to a *dynamic* equilibrium, without supposing any analogy with a *thermodynamic* one. Instead, η was defined in the broadest sense of simply giving some measure of the degree of excitation of the system during a single tap. This loose definition makes finding the precise relationship with Γ difficult. Nonetheless it is still possible to predict the overall shape of $\eta(\Gamma)$, as we now argue.

For η to be non-zero, the particles must at the very least separate from their nearest neighbours. Experiments on vibrated granular systems often claim to find

some critical Γ_c such that the relative motion of the particles is either minimal or non-existent for $\Gamma < \Gamma_c$ (usually $1 \lesssim \Gamma_c \lesssim 2$, see *e.g.* [1,8,38]). A facile explanation for this is to suppose that a granular body is held together by frictional forces, and that relative motion between adjacent particles is not possible until some static friction threshold has been overcome. Since all the normal contact forces are proportional to g, the distribution of threshold forces will also scale with g and thus the relevant parameter would indeed be $\Gamma = a_{\max}/g$. However, friction is not the only relevant mechanism. For instance, particle separation will still occur in vertical one dimensional columns, where friction clearly plays no part. Even in this case theory suggests that the relevant parameter is again Γ, at least in the limit of hard spheres [39].

Assuming that a well-defined Γ_c exists, the overall shape of $\eta(\Gamma)$ will obey $\eta(\Gamma) \approx 0$ for small Γ, only significantly deviating from zero for $\Gamma \gtrsim \Gamma_c$. Just this qualitative behaviour has been found in simulations of horizontally vibrated systems [40]. As a corollary, the annealing curves presented in Figs. 4 and 5 will be flatter for small Γ when plotted against Γ rather than η, in better agreement with the experimental graphs [9,10].

2. The prior distribution $\mu(E)$

The Gaussian and exponential $\mu(E)$ employed in the simulations were chosen as plausible first guesses of the real $\mu(E)$. To calculate the actual $\mu(E)$ is a non-trivial problem, but a first step might be to re-express $\mu(E)$ in terms of $\psi(\bar{v_f})$, the distribution of free volume after reconfiguration. Using $E = z^* \Delta E = A v_g / \bar{v_f}$ (3), this gives

$$\mu(E) = \frac{A v_g}{E^2} \, \psi \left(\frac{A v_g}{E} \right) \quad . \tag{13}$$

In principle, $\psi(\bar{v_f})$ could be found from a microscopic model, such as the parking lot model [9,17–19], for which the free volume is also the void volume.

Note that, from (13), the tail of $\mu(E)$, which is so important to the long-time relaxational properties of Bouchaud's trap model, can be related to the $\bar{v_f} \to 0^+$ behaviour of $\psi(\bar{v_f})$. For example, if $\psi(\bar{v_f})$ vanishes according to $\psi(\bar{v_f}) \sim \exp(-\alpha/\bar{v_f})$, then $\mu(E)$ will have an exponential tail and the trap model predicts a glass transition at a finite noise intensity $\eta = A v_g / \alpha$. Similarly, $\psi(\bar{v_f}) \sim \exp(-\alpha/\bar{v_f}^2)$ corresponds to a $\mu(E)$ with a Gaussian tail.

3. The constant $A = a \Delta E$

Even though A has been treated as an arbitrary constant and fixed by the initial conditions, its component factors a and ΔE have a physical interpretation, as we now discuss. In (3), a is defined as the constant of proportionality between z^*, the smallest number of particles that can cooperatively rearrange, and the ratio $v_g/\bar{v_f}$. In the Chicago group's original argument [9], a was set to 1; however, we prefer not to fix a at any particular value and suggest that it may depend upon particle properties such as their shape. For instance, highly irregular particles will obstruct motion more effectively than rounder particles of the same volume, and so should have a higher value of a.

ΔE was originally defined as a gravitational potential energy barrier. Indeed, assuming that the particles interact via hard core repulsion, this is the *only* available potential energy scale in the system. This suggests that ΔE is proportional to the mean vertical displacement between adjacent particles. If so, then our implicit assumption that ΔE is independent of η and ρ is compatible with the hard sphere Monte Carlo simulations of Barker and Mehta [41], who demonstrated that the distribution of contact angles between particles is roughly constant over a wide range of shaking amplitudes.

More importantly, if ΔE is gravitational potential energy, then inspection of the reconfiguration rate (6) indicates that η must also have units of energy, with an energy scale that is presumably coupled to the driving. For definiteness, suppose η can be written as $\eta = mgA_0 f(\Gamma)$, where m is the typical mass of the particles, A_0 is the amplitude of the driving and $f(\Gamma)$ is some function of the dimensionless parameter $\Gamma = a_{\max}/g$ (possibly with a threshold around $\Gamma \approx \Gamma_c$ as discussed earlier). Similarly, write $\Delta E \sim mgr$, where r is the typical particle radius. Since ΔE and η only appear in the ratio $\Delta E/\eta$, m and g will cancel and the dynamics of the model will depend on *two* dimensionless quantities, namely Γ and a dimensionless *displacement* A_0/r. The existence of a second relevant dimensionless parameter implies that the behaviour in response to high amplitude, low frequency driving may be qualitatively different from a low amplitude, high frequency driving with the same value of Γ. This possibility has not yet been explored in the experiments, which seem to have focused on the low frequency regime.

Note that we could equally have expressed η in terms of the kinetic energy supplied by the driving, *i.e.* $\eta = m v_0^2 \tilde{f}(\Gamma)$, where v_0 is the typical driving velocity. However, this is not an independent energy scale as v_0 can be dimensionally related to $a_{\max}$ and A_0 by $v_0 \sim \sqrt{a_{\max} A_0}$. We only mention this latter alternative because simulations often show scaling plots in terms of Γ and v_0 (see *e.g.* [40] and references therein).

V. SUMMARY AND CONCLUSIONS

To summarise, we have constructed a simple model for weakly excited granular media that combines the Chicago group's free volume argument with elements of the supercooled liquid theory of Adam and Gibbs. Integration of the master equation has shown that the model behaves

in a similar manner to the experiments for each of the situations considered. Some slight discrepancies remain with the power spectra, but these may be due to mechanisms currently lacking from the model, such as ordering effects and crystallinity, depth dependency or wall effects. It would be interesting to see if any of these mechanisms could be incorporated into an extended version of model. It may also be possible to introduce orientational degrees of freedom and compare the results to recent experiments on nylon rods [42].

The model has also been used to predict the manner in which the time of the peak response to a shift in Γ at $t = t_0$ scales with t_0, as discussed in Sec. III C. This prediction could be tested experimentally and may help to differentiate between the large number of models that have so far been proposed [12–25], as it seems unlikely that they will all give the same scaling behaviour. Further insight into the physical mechanisms underlying the compaction process could be gained by measuring the typical size of reconfiguring regions as a function of time, or by seeing if the locations of such regions are spatiotemporally correlated. Such measurements could be performed in simulations, or by direct visualisation of two dimensional experiments [43], for instance.

Finally, we note that the relationship between granular media and glasses can be given a more intuitive appeal by the following simple argument. Consider sand poured from a great height into a container. When the particles first hit the surface of the forming sandpile, the direction in which they bounce will essentially be random, giving rise to a large random velocity component. This corresponds to a highly excited state with (in our notation) a high η. However, the particles will rapidly lose their kinetic energy by inelastic collisions and will soon come to rest, jamming under gravity into a static, disordered configuration with $\eta = 0$. It is not difficult to see how this sequence of events can be related to the rapid 'quench' of a supercooled liquid or other glass-forming material.

Just after the initial submission of this work, we became aware of a master equation for the glass transition due to Dyre [44], which is similar to Bouchaud's equation studied in this paper but with a built-in cut-off in the range of allowed energies. Also, it has been brought to our attention that the two regimes of vibration mentioned in Sec. IV 3 have previously been discussed in the context of size segregation by Mehta and Barker [45].

ACKNOWLEDGEMENTS

The author would like to thank Mike Cates for helpful discussions and careful reading of the manuscript, and also Joachim Wittmer, Mario Nicodemi, Alan Bray, Jean-Philippe Bouchaud, Robin Stinchcombe and Suzanne Fielding for stimulating discussions on the experiments and this model. We would also like to thank Jeppe Dyre for bringing our attention to reference [44], and Anita Mehta and Gary Barker for reference [45]. This work was funded by UK EPSRC grant no. GR/M09674.

APPENDIX A: SIMULATION DETAILS

The bulk of the simulation results were obtained by numerical integration of the continuous master equation (9). $P(E,t)$ was defined on a mesh of points $P_{ij} = P(i\,\delta E, j\,\delta t)$, where $0 \le i \le i_{\max}$ and $j \ge 0$. Care was taken to ensure that $E_{\max} \equiv i_{\max}\,\delta E$ was set sufficiently high that there was no significant cut-off to $P(E,t)$ for large E. To iterate over a single time step δt, $\omega(t)$ was found from numerical integration of (9b) and then assumed to remain constant over the required time interval. This allowed the time evolution equation (9a) to be solved and P_{ij+1} found from P_{ij} $\forall i$. The whole distribution was then renormalised by a factor $(\sum_i P_{ij})^{-1}$ to correct for the non-conservation of probability resulting from the assumption of a constant $\omega(t)$. For relaxation under constant η, simulation times were improved by employing a geometric mesh with a linearly increasing time step $\delta t \propto t$. This allowed for times up to $t = 10^{10}$ to be reached with only modest CPU time.

For the density fluctuations investigated in Sec. III D, the continuous master equation was of no use and an alternative method was employed which explicitly included finite size effects. This involved assigning N array elements a barrier $E_{\rm i}$, $i = 1 \ldots N$, according to the chosen initial conditions. At every time step $\delta t = 1$, each element was assigned a new barrier with probability $\omega_0\,\mathrm{e}^{-E_i/\eta}$, where the new barrier values were drawn from the prior $\mu(E)$. The density ρ_i of each element was found by inverting the mapping (7), and the mean density calculated by straightforward summation, $\rho(t) = \frac{1}{N}\sum \rho_i$.

APPENDIX B: MONOTONICITY OF $\rho_\infty(\eta)$ ON η

In this appendix it is shown that the asymptotic density $\rho_\infty = \lim_{t\to\infty}\rho(t)$ is a monotonic decreasing function of η for essentially any $\mu(E)$. If an equilibrium state exists, it takes the form $P_{\rm eqm}(E) = \omega_\infty(\eta)\,\mathrm{e}^{E/\eta}\mu(E)$ and hence from (8),

$$\frac{\rho_\infty(\eta)}{\rho_{\max}} = 1 - \int_0^\infty \frac{\omega_\infty(\eta)\mathrm{e}^{E/\eta}\mu(E)}{1 + E/A\rho_{\max}}\,\mathrm{d}E \ , \tag{B1}$$

$$\omega_\infty(\eta) \equiv \lim_{t\to\infty}\omega(\eta,t) = \left(\int_0^\infty \mathrm{e}^{E'/\eta}\mu(E')\,\mathrm{d}E'\right)^{-1} . \tag{B2}$$

Differentiating (B1) with respect to η and rearranging gives

$$\frac{\eta^2}{\omega_\infty^2(\eta)\,\rho_{\max}}\frac{\partial\rho_\infty(\eta)}{\partial\eta} = \int_0^\infty\int_0^\infty (E-E')\frac{\mu(E)\mu(E')\mathrm{e}^{(E+E')/\eta}}{1+E/A\rho_{\max}}\,\mathrm{d}E\,\mathrm{d}E' \ . \tag{B3}$$

After the change of variables $u = E + E'$ and $v = E - E'$ and substituting $v \to -v$ over the domain $v < 0$, the right hand side of (B3) transforms to

$$- \int_{u=0}^{\infty} \int_{v=0}^{u} v^2 \, \mathrm{e}^{u/\eta} \mu\left(\frac{u+v}{2}\right) \mu\left(\frac{u-v}{2}\right) \times \Big[(2A\rho_{\max} + u + v)(2A\rho_{\max} + u - v)\Big]^{-1} \, \mathrm{d}u \, \mathrm{d}v \ . \quad \text{(B4)}$$

Since all the factors inside the integral (B4) are positive, it can be trivially deduced that

$$\frac{\partial \rho_{\max}}{\partial \eta} \leq 0 \qquad \text{for all } \eta. \quad \text{(B5)}$$

Equality is attained in only two cases. The first is if the integrand is strictly zero over the entire range $v > 0$, which can only happen in the trivial case of a single valued distribution $\mu(E) = \delta(E - E_0)$. The second and more important situation is over a range of η for which no equilibrium state exists. In this case, all the moments of $P(E,t)$ diverge as $t \to \infty$ and $\rho(t) \to \rho_{\max}$ from (7). A plot of $\rho_\infty(\eta)$ versus η for an exponential and a Gaussian $\mu(E)$ is given in Fig. 12.

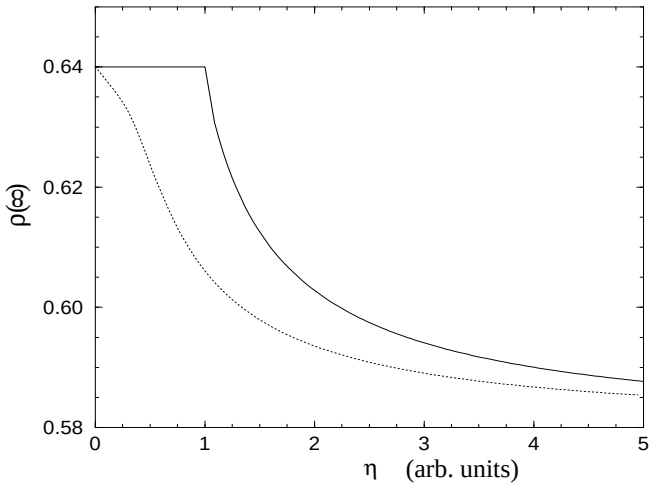

FIG. 12. Plot of $\rho_\infty \equiv \lim_{t\to\infty} \rho(t)$ against η for an exponential $\mu(E) = \mathrm{e}^{-E}$ (solid line) and the Gaussian $\mu(E) = \sqrt{2/\pi}\mathrm{e}^{-E^2/2}$ (dotted line) for $\rho_{\max} = 0.64$. Note that the plateau for $\eta \leq 1$ in the exponential case corresponds to the out-of-equilibrium situation where all the moments of $P(E,t)$ diverge as $t \to \infty$.

APPENDIX C: ANALYSIS OF THE POWER SPECTRA

The small f behaviour of the power spectra of density fluctuations $S(f)$ is analytically derived in this appendix, which extends the range of the numerical observations discussed in Sec. III D. The time-dependent spectrum near the glass point has already been derived in [30]; here we consider the $f \to 0^+$ limit in equilibrium for general $\mu(E)$ over a wider range of η.

Since each local region is assumed to relax independently of its environment, the total power spectrum $S(f)$ is just the spectrum for a single region with a relaxation time τ averaged over $\Phi(\tau)$, the distribution of relaxation times in equilibrium,

$$S(f) \propto \int \frac{\tau \, \Phi(\tau)}{1 + (2\pi f \tau)^2} \, \mathrm{d}\tau \ . \quad \text{(C1)}$$

The small f behaviour of (C1) depends on the asymptotic behaviour of $\Phi(\tau)$ for large τ. If $\Phi(\tau)$ decays faster than τ^{-2}, then the $f \equiv 0$ limit exists and $S(f)$ exhibits the expected $1/f^0$ noise for low frequencies. However, if $\Phi(\tau) \sim \tau^{-x}$ with $1 < x < 2$, then $S(f) \sim 1/f^{2-x}$, as can be readily seen by substituting for $f\tau$ in (C1) (note that $x > 1$ since $\Phi(\tau)$ is normalisable).

For the trap model, $\Phi(\tau)$ can be found for any given $\mu(E)$ by simply making the change of variables $\tau = \frac{1}{\omega_0}\mathrm{e}^{E/\eta}$ into the expression for $P_{\mathrm{eqm}}(E)$, equation (10). Thus, an exponential $\mu(E) \sim \mathrm{e}^{-E/\eta_{\mathrm{g}}}$ gives $\Phi(\tau) \sim \tau^{-\eta/\eta_{\mathrm{g}}}$, implying that $S(f) \sim 1/f^{2-\eta/\eta_{\mathrm{g}}}$ for $\eta_{\mathrm{g}} < \eta < 2\eta_{\mathrm{g}}$. This confirms that $S(f) \not\to 1/f^0$ for this range of η, even though the system is in equilibrium. The usual $1/f^0$ behaviour is recovered when $\eta \geq 2\eta_{\mathrm{g}}$, which also applies for all η when $\mu(E)$ decays faster than exponentially. In particular, a Gaussian $\mu(E) \sim \mathrm{e}^{-E^2/2\sigma^2}$ leads to an equilibrium distribution of relaxation times of the form

$$\Phi(\tau) \sim \tau^{-\frac{\eta^2}{2\sigma^2}\ln(\omega_0\tau)} \ , \quad \text{(C2)}$$

which is suggestive of a power law with a slowly varying exponent $x = \frac{\eta^2}{2\sigma^2}\ln(\omega_0\tau)$. Thus one would expect $S(f)$ to exhibit approximate power law behaviour over a wide range of f, reverting to $1/f^0$ only for frequencies comparable to the 'largest' relaxation time $\omega_0\tau^* \sim \mathrm{e}^{\sigma^2/\eta^2}$. Any attempt to fit $S(f)$ to a power law will give an exponent that depends on the range of f considered as well as the ratio η/σ.

* Electronic address: david@ph.ed.ac.uk

[1] H. M. Jaeger, S. R. Nagel and R. P. Behringer, Rev. Mod. Phys. **68**, 1259 (1996).

[2] H. M. Jaeger and S. R. Nagel, Science **255**, 1523 (1992).

[3] M. D. Ediger, C. A. Angell and S. R. Nagel, J. Phys. Chem. **100**, 13200 (1996).

[4] C. A. Angell, Science **267**, 1924 (1995).

[5] J. Hammann, E. Vincent, V. Dupuis, M. Alba, M. Ocio and J.-P. Bouchaud, to appear in the proceedings of the *Frontiers in Magnetism* workshop, Kyoto (1999), also *cond-mat/9911269*.

[6] J.-P. Bouchaud, to appear in the proceedings of the *Soft and fragile matter* summer school , St. Andrews (1999), also *cond-mat/9910387*.
[7] S. Nagata, P. H. Keesom and H. R. Harrison, Phys. Rev. B **19**, 1633 (1979).
[8] J. B. Knight, C. G. Fandrich, C. N. Lau, H. M. Jaeger and S. R. Nagel, Phys. Rev. E **51**, 3957 (1995).
[9] E. R. Nowak, J. B. Knight, E. Ben-Naim, H. M. Jaeger and S. R. Nagel, Phys. Rev. E **57**, 1971 (1998).
[10] E. R. Nowak, J. B. Knight, M. L. Povinelli, H. M. Jaeger and S. R. Nagel, Powder Technology **94**, 79 (1997).
[11] C. Josserand, A. Tkachenko, D. M. Mueth and H. M. Jaeger, *"Memory effects in granular material,"* preprint (2000), also *cond-mat/0002401*.
[12] E. Caglioti, V. Loreto, H. J. Herrmann and M. Nicodemi, Phys. Rev. Lett. **79**, 1575 (1997).
[13] M. Nicodemi, A. Coniglio and H. J. Herrmann, Phys. Rev. E **55**, 3962 (1997).
[14] M. Nicodemi and A. Coniglio, Phys. Rev. Lett. **82**, 916 (1999).
[15] M. Nicodemi, *"Domains growth and packing properties in driven granular media subject to gravity,"* preprint (1999), also *cond-mat/9911338*.
[16] M. Nicodemi, Phys. Rev. Lett. **82**, 3734 (1999).
[17] A. Prados, J. J. Brey and B. Sánchez-Rey, *"Hysteresis in vibrated granular media,"* to appear in Physica A (2000), also *cond-mat/9912237*.
[18] A. J. Kolan, E. R. Nowak and A. V. Tkachenko, Phys. Rev. E **59**, 3094 (1999).
[19] J. Talbot, G. Tarjus and P. Viot, *"The adsorption-desorption model and its application to vibrated granular materials,"* preprint (1999), also *cond-mat/9910239*.
[20] K. L. Gavrilov, Phys. Rev. E **58**, 2107 (1998).
[21] D. A. Head and G. J. Rodgers, J. Phys. A **31**, 107 (1998).
[22] S. Luding, M. Nicolas and O. Pouliquen in *Compaction of Soils, Granulates and Powders*, edited by D. Kolymbas and W. Fellin (Balkema, Rotterdam, 2000), also *cond-mat/0003172*.
[23] S. F. Edwards and D. V. Grinev, Phys. Rev. E **58**, 4758 (1998).
[24] S. Linz, Phys. Rev. E **54**, 2925 (1996).
[25] A. Mehta and G. Barker, *"Glassy dynamics in granular compaction,"* to appear in J. Phys.: Cond. Mat. (2000), also *cond-mat/9912077*.
[26] T. Boutreux and P. G. de Gennes, Physica A **244**, 59 (1997).
[27] G. Adam and J. H. Gibbs, J. Chem. Phys. **43**, 139 (1965).
[28] M. H. Cohen and D. Turnbull, J. Chem. Phys. **31**, 1164 (1959).
[29] J.-P. Bouchaud, J. Phys. I **2**, 1705 (1992).
[30] J.-P. Bouchaud and D. S. Dean, J. Phys. I **5**, 265 (1995).
[31] J.-P. Bouchaud, A. Comtet and C. Monthus, J. Phys. I **5**, 1521 (1995).
[32] C. Monthus and J.-P. Bouchaud, J. Phys. A **29**, 3847 (1996).
[33] Anonymous, Nature **239**, 488 (1972).
[34] P. Granberg, L. Sandlund, P. Nordblad, P. Svedlindh and L. Lundgren, Phys. Rev. B **38**, 7097 (1988).
[35] M. Sasaki and K. Nemoto, *"Scaling law and aging phenomena in the random energy model,"* preprint (2000), also *cond-mat/0002021*.
[36] C. S. Campbell, Ann. Rev. Fluid Mech. **22**, 57 (1990).
[37] A. Mehta and S. F. Edwards, Physica A **157**, 1091 (1989).
[38] E. E. Ehrichs, H. M. Jaeger, G. S. Karczmar, J. B. Knight, V. Y. Kuperman and S. R. Nagel, Science **267** 1632 (1995).
[39] T. Pöschel, T. Schwager and C. Salueña, *"Onset of fluidization in vertically shaken granular material,"* preprint (1999), also *cond-mat/9711234 v2*.
[40] G. H. Ristow, G. Straßburger and I. Rehberg, Phys. Rev. Lett. **79**, 833 (1997).
[41] G. C. Barker and A. Mehta, Phys. Rev. E **47**, 184 (1993).
[42] F. X. Villarruel, B. E. Lauderdale, D. M. Mueth and H. M. Jaeger, *"Compaction of rods: Relaxation and ordering in vibrated, anisotropic granular material,"* preprint (2000), also *cond-mat/0001457*.
[43] S. Warr, J. M. Huntley and G. T. H. Jacques, Phys. Rev. E **52**, 5583 (1995).
[44] J. C. Dyre, Phys. Rev. Lett. **58**, 792 (1987).
[45] G. C. Barker and A. Mehta, Nature **364**, 486 (1993).